Reactive mass transport modelling in discretely-fractured porous media

N.F. Ghogomu & R. Therrien
Département de géologie et génie géologique, Université Laval, Québec, Canada

ABSTRACT: This paper presents a model that simulates groundwater flow and multispecies transport in discretely-fractured porous media. The porous matrix is discretized with three-dimensional elements, and discrete fractures are represented by two-dimensional planar elements. Superposition of fracture and matrix nodes ensures fluid and mass continuity. Advective-dispersive transport is coupled with reactive transport for chemical species that undergo either chemical equilibrium or kinetic reactions. The chemical system is defined mathematically with the law of mass action applied to each chemical reaction, and the mass conservation law to each basic chemical component. The resulting nonlinear algebraic system of equation is solved with the Newton-Raphson technique, and a sequential iterative approach couples the physical and chemical transport equations. A verification example involving simple mineral dissolution is presented. A second example with precipitation and dissolution of minerals illustrates the influence of discrete fractures and matrix diffusion on the spatial distribution of reactive chemical species.

1 INTRODUCTION

Several field and laboratory studies have revealed that a detailed description of chemical systems, as well as the consideration of physical migration of chemical species, are necessary to simulate reactive transport in the subsurface. Examples include the fate of biodegradable organic contaminants in the subsurface, or the impact of acid mine drainage on groundwater quality. These problems are now tackled with multicomponent transport simulators, which treat chemical interactions rigorously, as opposed to a simplified representation such as that provided by a first-order decay term. In contrast to non-reactive models, the need for efficient numerical techniques is enhanced for the field-scale application of multicomponent models, because several thousands of nodes can be required, with several unknowns (chemical species) at each node. An example is the field-scale simulation of acidic mine discharge into an aquifer, presented by Walter et al. (1994), where the fate of over 40 chemical species is simulated for a finite element grid containing more than 10000 nodes.

Steefel & MacQuarrie (1996) present a detailed description of reactive mass transport modelling. They describe basic ingredients in modelling reactive mass transport and present various solutions methods for specific chemical reactions. Physical transport, advection-dispersion, is described with a set of partial differential equations for each mobile chemical component. Reaction systems are then defined by a set of nonlinear algebraic equations. These equations arise from the application of the law of mass action for the chemical reaction (equilibrium or kinetic) and mass conservation for chemical components. The chemical components are obtained by using the concept of basis from vector algebra, from which all chemical species can be defined. Steefel & MacQuarrie (1996) describe the algebra required to obtain the canonical formulation for the chemical equations, or its equivalent, which is the tableaux form of Morel (1983).

One possible method to solve the reactive transport problem is to fully couple physical and reactive transport. This approach, which is also called the direct method, requires incorporating all relevant chemical reactions in a multicomponent system directly into the physical transport equations. Chemical reactions thus constitute non-linear source and sink terms in the transport equation. Leeming et al. (1998) have used a fully-coupled model for reactive transport. One advantage of fully coupling is that, when used in conjunction with an implicit temporal discretization, there is no stability criteria for the time step size. However, the computational work per time step is very high to solve the fully coupled non linear system of equations. Furthermore, the core memory requirement can be extremely high for large

problems (large number of nodes and chemical species), which might prevent the use of the method.

The two-step method, also termed the sequential iteration approach, represents an alternative to the fully-coupled method. The physical transport equations are spatially connected, but the chemical reactions depend only on local conditions at each time step and at each point in the system, and do not show spatial connection. When no spatial connection is assumed for the chemical reactions, they can be solved separately from the physical transport equations. The two-step method therefore divides the solution into a physical transport step and a chemical step. During the transport step, aqueous species migrate individually by advection and dispersion, while in the chemical step chemical species react with each other. Transport and chemistry can be coupled sequentially or iteratively. Liu & Narasimham (1989), Engesgaard & Kipp (1992), and Schäfer et al. (1998), among others, have used two-step methods for reactive transport modelling. Solving physical and reactive transport separately greatly reduces the memory requirements for the model. Another advantage is that, since the advection-dispersion equation and the chemical reaction equations have different mathematical properties, different methods can be tailored for their solution. For very large problems, the sequential iteration approach might be the only one feasible because of the extreme memory requirements for the fully-coupled approach.

Among the reactive transport models that have been presented in the past, there are few that explicitly consider fractures present in geological materials. Since fractures located in geologic materials can greatly influence the reactive mass transport process, and can represent preferential pathways for solute migration, they need to be considered. Various conceptual models exist to represent fractured media (for example: equivalent porous medium, porous medium with double porosity, and discretely-fractured porous medium approach). For solute transport in fractured media, velocities in fractures are often relatively high, but contaminant diffusion from the fractures to the porous matrix can significantly reduce migration rates along the fractures. Furthermore, Steefel & Lichtner (1998a) state that the geochemical and hydrogeological conditions in groundwater systems in some fractured materials are characterized by spatial heterogeneity, large numbers of aqueous and chemical species, species concentration ranging over several orders of magnitude, and multiple sharp fronts separating mineral distribution or zone of distinct geochemistry. For cases where diffusion is important, discrete fracture models for mass transport in fractured media are needed, such as that presented by Therrien & Sudicky (1996).

Recognizing that fractures need to be explicitly accounted for, and that an equivalent porous medium approach is not suitable, Steefel & Lichtner (1994), Novak (1996), and Steefel & Lichtner (1998a,b) have presented simulations of reactive transport in discretely-fractured porous media. The motivation of their work is to understand the control on reactive contaminant transport near waste repositories and determine mineral distribution in fractured systems. Steefel & Lichtner (1994) and Steefel & Lichtner (1998a) presented a one and two-dimensional model including physical transport and reaction. They considered that transport within the porous matrix was only via molecular diffusion. Steefel & Lichtner (1998a) derived a dimensionless parameters to relate the relative position of reactive fronts in the fracture and the matrix, for a simple case.

The objective of the work presented here is to develop a numerical model that can simulate multicomponent transport in discretely-fractured porous media. The physical transport model is that of Therrien & Sudicky (1996), which solves 3D flow and mass transport in both a porous matrix and a set of discrete fractures. The chemical reactions are treated according to the method presented by Schäfer et al. (1998). A two-step iterative method is used to couple physical and reactive transport. This paper summarizes the mathematical and numerical formulations, it also presents a verification example for reactive transport and a simple illustrative problem for a discretely-fracture porous medium.

2 PHYSICAL AND CHEMICAL SYSTEM

The discrete fracture conceptual model is adopted for representing the porous medium. The physical system therefore consists of a porous matrix that is intersected by planar fractures. Flow and transport can occur in both the porous matrix and the fractures, which implies that the matrix is not impermeable. The fluid is essentially incompressible, its density is constant, and isothermal conditions prevail. Fully saturated flow conditions are assumed. Furthermore, the fractures and the porous matrix are non-deformable.

The fractures are idealized as two-dimensional plates, which implies uniform hydraulic head and concentration across the fracture width. For the physical system considered, the hydraulic conductivity of the fractures, given by the cubic law, is much higher than that of the porous matrix. Advection of solute will therefore be primarily along the fractures, while the main transport process in the porous matrix will be molecular diffusion.

The chemical system is described with the method of components proposed by Morel (1983). For a system containing N_s chemical species, a set of N_c components is identified and represents the basis from which all chemical species can be defined. A mass conservation equation is written for each com-

ponent. The mathematical definition of the chemical system is completed by identifying N_r chemical reactions, such as complexation, precipitation and dissolution reactions. Equilibrium or first-order kinetic reactions can be considered. The final system of non-linear algebraic equations, needed to solve for the concentration of the N_s species, contains $N_c + N_r$ equations (where $N_s = N_c + N_r$).

The chemical reactions can occur in both the fractures and the porous matrix. Although mineral precipitation and dissolution have been shown to influence the physical properties of the porous medium and fracture (Steefel & Lichtner 1998a), this effect is not considered here.

3 GOVERNING EQUATIONS

3.1 *Advective-dispersive transport*

To represent flow and transport in discretely-fractured porous media, where the matrix is not impermeable, equations are needed for both the fracture and the matrix. A detailed presentation of the governing equations for 3D variably-saturated groundwater flow and solute transport in a discretely-fractured porous media can be found in Therrien & Sudicky (1996). Similar equations are used here, except that only saturated flow conditions are considered. Saturated 3D flow in the porous matrix is described by:

$$\frac{\partial}{\partial x_i}\left(K_{ij}\frac{\partial h}{\partial x_j}\right) \pm Q = S\ \frac{\partial h}{\partial t} \quad i,j = 1,2,3 \tag{1}$$

where K_{ij} is the saturated hydraulic conductivity of the porous matrix, h is the matrix hydraulic conductivity, and S_s is the specific storage. Fluid sources and sinks, such as exchange with the fractures, are represented by Q, and i and j are spatial coordinates.

Because of the parallel plate approximation for flow and transport in a fracture, the governing equation for the fracture will be in two dimensions as opposed to the three-dimensional matrix equation. Flow into the fracture is described by:

$$\frac{\partial}{\partial x_i}\left(2b\frac{\partial h_f}{\partial x_j}\right) - q_n \pm Q_f = (2b)\frac{\partial h_f}{\partial t} \quad i,j = 1,2 \tag{2}$$

where subscript f refers to the fracture, $2b$ is the fracture aperture, Q_f is a general source or sink term, and q_n is the fluid leakage term between the fracture and the matrix.

The advection-dispersion equation, including a reaction term, is also needed for both the matrix and the fracture system. If components are used to define all chemical species, the advection-dispersion equation only needs to be written for each component and not for each chemical species. One condition is that the components have transport properties (for example: diffusion coefficient, partition coefficient or decay constant) that are similar to those of the chemical species. If the condition is met, there will be savings in computation since the number of components (N_c) is always smaller than the number of chemical species (N_s). For each component, the matrix transport equation is:

$$R\frac{\partial c}{\partial t} + q_i\frac{\partial c}{\partial x_i} - \frac{\partial}{\partial x_i}\left(D_{ij}\frac{\partial c}{\partial x_j}\right) +$$

$$R\lambda c \pm S = 0 \quad i,j = 1,2,3 \tag{3}$$

where c is the component concentration, R is the retardation factor for the component, q is the fluid flux obtained from Darcy's law, D_{ij} is the hydrodynamic dispersion tensor, and λ is a first-order decay constant. Variation in the concentration of a component, which results from chemical reactions, is represented by S in equation (3). A second equation describes 2D transport in the fractures:

$$2b\left[R_f\frac{\partial c_f}{\partial t} + q_{fi}\frac{\partial c_f}{\partial x_i} - \frac{\partial}{\partial x_i}\left(D_{fij}\frac{\partial c_f}{\partial x_j}\right)\right] +$$

$$2bR_f\lambda c_f \pm S = 0 \quad i,j = 1,2 \tag{4}$$

where the component concentration in the fracture is given by c_f, and R_f, q_f and D_f are the retardation factor, the fluid flux, and the dispersion coefficient in the fracture, respectively.

3.2 *Reactive transport*

The chemical reactions, represented by S in equations (3) and (4), are described in a fashion identical to that proposed by Schäfer et al. (1998). Reference to Schäfer et al. (1998) is suggested for more details on the formulation. The model is general such that all reactions can be time-dependant and obey first-order kinetics. However, if the reaction time scale is much smaller than the time scale of solute transport, instantaneous equilibrium can be assumed. Calculation of the chemical equilibrium is based on the law of mass action. For each of the N_r reactions, the law of mass action has the following form:

$$\prod_i (a_i\, C_i)^{sc_{i,j}} - K_j \quad j = 1,\ldots,N_r \tag{5}$$

where a_i is the activity coefficient of chemical species i, $sc_{i,j}$ is its stoichiometric coefficient in reaction j, and K_j is the equilibrium constant for the reaction. The concentration of the chemical species, C_i, is in upper case, since it is not necessarily the same as the concentration appearing in equations (3) and (4). The equilibrium constant can be temperature dependent and expressed with the Van't Hoff equation (Stumm & Morgan 1981). For solution with a low

ionic strength, the activity coefficient is equal to 1 and the chemical equations are written in terms of concentrations. For higher ionic strengths, corresponding to a more concentrated solution, the activity coefficient of a species is determined from the Davies approximation equation (Stumm & Morgan 1981).

Mass conservation of each of the N_c components is given by:

$$\sum_m \left(con_{m,n} \cdot C_m\right) - COMP_n = 0 \quad n = 1,..., N_c \tag{6}$$

where $con_{m,n}$ is the contribution of species m to component $COMP_n$ in the mass conservation equation.

When applicable, kinetic reactions are treated as coupled forward and backward equilibrium reactions, with rate constants equal to k_1 and k_2, respectively. Only the forward reaction plays a role for an irreversible kinetic reaction. The following general form defines the first-order kinetic reaction for species m:

$$\frac{\partial C_m}{\partial t} = k_1 \cdot \prod_i \left(a_i\, C_i\right)^{sc_i} + k_2 \cdot \prod_j \left(a_j\, C_j\right)^{sc_j} \tag{7}$$

where C_m is the concentration of species m, C_i and C_j are the concentrations of those species which affect the kinetics of the reaction, and sc is their stoichiometric coefficients in the reactions.

Similarly to the model of Schäfer et al. (1998), the complete chemical system (species, reactions and components) is defined by the user, instead of coupling the physical transport model to a geochemical database. Also, mineral dissolution is allowed only if the concentration of the mineral is greater than zero.

4 NUMERICAL FORMULATION

The model presented here is based on that of Therrien & Sudicky (1996), which solves the flow and transport equations for discretely-fractured porous media. The model uses a standard Galerkin finite element method for discretization of flow and solute transport equations in the solid matrix and in the discrete fracture. The porous matrix is discretized with three-dimensional elements, and fractures are represented by two-dimensional planes. Nodes forming the fractures are superposed onto matrix nodes. These coincident nodes have similar hydraulic conductivity and concentration, which eliminates the direct calculation of the matrix/fracture exchange terms in equations (2) and (4). An option exists for using a finite difference representation for the governing equations by modifying the elemental matrices (Therrien & Sudicky 1996). Spatial representation of the advective term is either by upstream or central weighting. Fully implicit schemes can be selected for temporal discretization. The overall matrix equations are solved with a preconditioned iterative solver (VanderKwaak et al. 1995).

The chemical system contains N_s non linear equations (N_c mass balance equations and N_r reactions). The overall algebraic equation system for chemistry is solved with the Newton-Raphson method.

The whole equation system describing flow, transport and chemistry is solved in a sequential manner. Flow is solved first, either for steady-state or transient conditions. The physical and chemical transport are decoupled and solved with an iterative two-step procedure (Schäfer et al. 1998). The advective and dispersive transport equations are solved independently for each species or aqueous component. The source/sink terms accounting for chemical reactions are taken explicitly, with values from the preceding time step, to solve the physical transport. The chemical reaction equations are solved with the concentration changes from the transport step as explicit source/sink terms. For any given time-step, iteration between the physical and chemical solutions is conducted, until a maximum number of iteration is reached or until convergence of this two-step procedure.

5 VERIFICATION AND EVALUATION OF THE MODEL

No closed-form solution exists for multicomponent transport in discretely-fractured media, for either equilibrium or kinetic reactions. Verification of the present model must therefore rely on comparison with other numerical models. Ghogomu & Therrien (1999) present verification examples for multicomponent transport in nonfractured media, for cases where equilibrium or kinetic reactions are considered.

A verification example of equilibrium mineral dissolution is first presented to show that the model reproduces previously published results (Liu & Narasimhan 1989). An illustrative example of multicomponent transport in a discretely-fractured porous medium follows the verification example. Two very simple fracture geometries are used for a multicomponent transport problem, with precipitation and dissolution of minerals.

5.1 *Dissolution of a mineral species*

Liu & Narasimhan (1989) used this first verification problem to test their numerical model. A hypothetical one-dimensional column, with unit cross section area, contains two aqueous species, A and B, and one solid phase, AB. The solid AB has a solubility product equal to 1, and the activities of the aqueous

species are assumed equal to their concentrations. No complexation between species is considered, and the only chemical reaction is the dissolution of AB, which is described by equation (8).

$$AB = A + B \tag{8}$$

The species are uniformly distributed along the column, with initial concentrations equal to 1 mol/l for A and B, and 2.0 mol/l for AB. The initial solution in the column is therefore saturated with respect to solid phase AB, since the product of concentrations A and B is equal to the equilibrium constant.

Three chemical species are present in the system and three equations are needed to solve for chemical equilibrium. Application of the law of mass action provides the first equation, while the remaining two equations result from mass balance applied to the two component, A and B.

Flow is at steady-state flow in the column. Starting at a time equal to zero, the composition of the incoming fluid (at x = 0 m) is modified, with concentration of species A equal to 0.5 mol/l and concentration of species B equal to zero. The incoming fluid is undersaturated with respect to solid AB, and dissolution of AB will occur in the column.

To simulate the transport of species A and B, and the dissolution of species AB, the column is discretized in one dimension. A total of 60 one-dimensional elements are used, with a uniform grid spacing equal to 0.0167 m. The saturated hydraulic conductivity of the material in the column is equal to 0.0007 m/year, its porosity is equal to 0.25, and the longitudinal dispersivity is equal to 0.001 m. The fluid velocity in the column is equal to 1 m/year.

To reproduce results from Liu & Narasimhan (1989), the injection of a half pore volume of fluid is simulated. Figure 1 shows the simulated concentration versus distance for aqueous phases A, B and mineral AB at the end of simulation.

The profiles of the aqueous phase concentration can be divided into three distinct regions as presented by Liu & Narasimhan (1989). The first region nearest to the upstream boundary marks the position of the dissolution front (between x = 0.0 m and x = 0.05 m). Mineral AB has dissolved and the concentrations of A and B equal that of the incoming fluid. The second region (between x = 0.05 m and x = 0.8 m) corresponds to the location of the advective-dispersive front. This region marks the transition between initial concentration for A and B (downstream) and the new equilibrium concentrations resulting from the invasion of the incoming fluid. These new equilibrium concentrations are equal to 1.281 mol/l and 0.781 mol/l for A and B, respectively. These values are the same as those provided by Liu & Narasimhan (1989). The third region, located at the end of the column (x > 0.8 m) has not yet been reached by the incoming fluid.

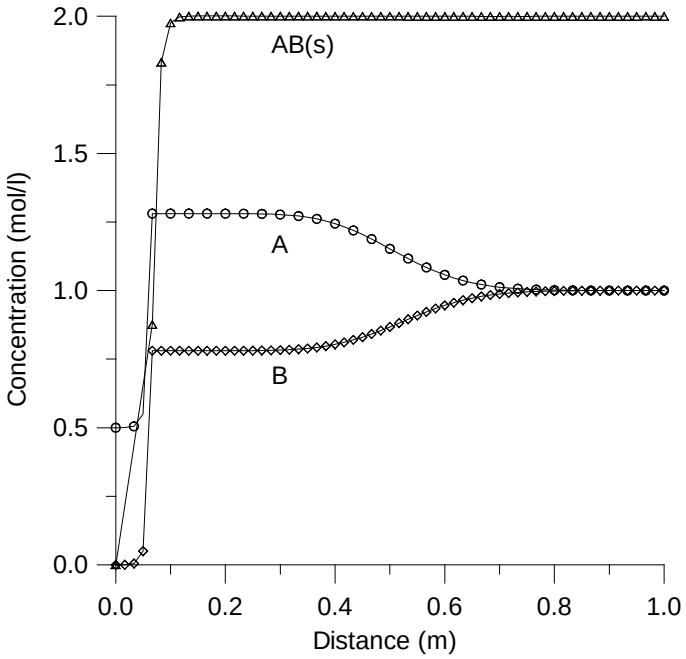

Figure 1. Results for the verification example showing concentrations after injection of one-half pore volume of fluid.

Although the equilibrium concentrations simulated here agree with those of Liu & Narasimhan (1989), a complete comparison of the concentration profiles is not possible. The reason is that Liu & Narasimhan (1989) simulated purely advective transport. Because of the numerical formulation used here, the dispersivities cannot be zero, which results in fronts that are more spread than those shown by Liu & Narasimhan (1989).

5.2 *Dissolution/precipitation in a fracture network*

This example illustrates multicomponent reactive transport in a discretely-fractured porous media. The physical system considered is two-dimensional, with lengths equal to 5m and 0.1 m in the x- and y-direction, respectively, and a unit thickness in the z-direction (Fig. 2).

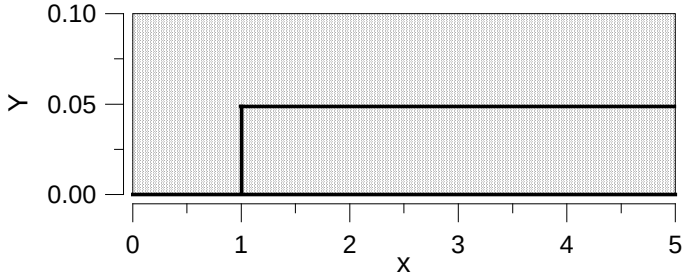

Figure 2. Geometry for the illustrative example. The fractures are indicated by thick lines.

The porous matrix has a hydraulic conductivity equal to 1×10^{-8} m/s and its porosity is equal to 0.5. Longitudinal and transverse dispersivity in the matrix are equal to 0.05 m and 0.005 m, respectively. The effective diffusion coefficient in the porous matrix, defined as the product of tortuosity and free

solution diffusion coefficient, is equal to 1×10^{-10} m^2/s.

Two different simulations are considered, based on two different fracture configurations. The first simulation (case A) is for a single main fracture located in the matrix. This fracture is oriented along the x-axis, it is located at y = 0 m and extends from x = 0 m to x = 5 m (Fig. 2). For the second simulation (case B), two additional fractures are considered along with the main fracture described above. A second fracture, parallel to the main fracture, is located at y = 0.05 m and extends from x = 1 m to x = 5 m. A third fracture, perpendicular to the first two fractures, is located at x = 1 m and extends from y = 0 m to y = 0.05 m. This third fracture connects the two previous ones. All fractures have uniform apertures equal to 5×10^{-6} m, which results in a hydraulic conductivity of 2×10^{-3} m/s. The longitudinal and lateral dispersivities of the fractures are 0.2 m and 0.02 m, respectively.

The chemical system for this problem is similar to that used by Engesgaard & Kipp (1992) in one of their verification examples. Table 1 lists the reactions considered in the chemical system, along with their equilibrium constants.

Table 1. Reactions and equilibrium constants

Reaction	log K_{eq}
$CaCO_3(s) = Ca^{2+} + CO_3^{2-}$	-8.47
$CaMg(CO_3)_2(s) = Ca^{2+} + Mg^{2+} + 2CO_3^{2-}$	-17.17
$H^+ + OH^- = H_2O$	14.01
$H^+ + CO_3^{2-} = HCO_3^-$	10.33
$H^+ + HCO_3^- = H_2CO_3$	6.3
$Ca^{2+} + CO_3^{2-} = CaCO_3(aq)$	3.23
$Mg^{2+} + CO_3^{2-} = MgCO_3(aq)$	2.98

The total number of chemical species is equal to 11. Since 7 reactions are defined, 4 components must also be identified to completely define the chemical system. These four components are defined in Table 2.

Table 2. Definition of components

Component	Definition
TOTCa	$CaCO_3(s) + CaMg(CO_3)_2(s) + Ca^{2+} + CaCO_3(aq)$
$TOTCO_3$	$CaCO_3(s) + CO_3^{2-} + HCO_3^- + H_2CO_3 + CaCO_3(aq) + MgCO_3(aq)$
TOTMg	$CaMg(CO_3)_2(s) + Mg^{2+} + MgCO_3(aq)$
TOTH	$H^+ - OH^- + HCO_3^- + 2\ H_2CO_3$

Rectangular elements are used to discretize the domain in two dimensions. A constant nodal spacing equal to 0.05 m and 0.005 m are used in the x and y direction, respectively. A total of 2000 elements constitute the finite element mesh. Steady-state flow conditions are simulated by imposing a constant hydraulic head equal to 0.5 m at the inflow boundary (located x = 0 m) and a lower hydraulic head equal to 0.0 m at the outflow boundary (located at x = 5 m). For case A, this hydraulic gradient results in a uniform fluid velocity equal to 2×10^{-4} m/s in the main fracture. For case B, the fluid velocity is variable in the main fracture. It increases to a value equal to 3.38×10^{-4} m/s for the section located between the inflow boundary (x = 0 m) and the intersection with the perpendicular fracture (x = 1 m). For the remainder of the main fracture (x > 1 m), the velocity decreases to about 1.7×10^{-4} m/s. Thus, keeping similar boundary conditions but including more fractures modifies velocities along the main fracture.

From the steady-state flow field, reactive transport is simulated in the column. Initial and boundary conditions for the components and mineral species are given in Table 3. Transport is simulated for 6 hours (14 400 s), with a constant time-step equal to 100 s.

Table 3. Initial and boundary conditions

Component	Initial	Inflow
Total Ca	1.239×10^{-4}	0.0
Total CO_3	1.239×10^{-4}	0.0
Total Mg	0.0	1.0×10^{-3}
Total H	-3.26×10^{-6}	-2.78×10^{-8}
$CaCO_3(s)$	2.17×10^{-5}	0
$CaMg(CO_3)_2(s)$	0.0	0
pH	7.06	9.91

Concentrations of component are in moles per litre of fluid and concentrations of minerals are in moles per kg of solid.

Figures 3-4 show the distribution of several chemical species along the main fracture located at y = 0 m for cases A and B. Figure 5 presents results in a direction perpendicular to this main fracture, which corresponds to a profile into the porous matrix downstream of the fracture oriented along the y axis.

Initially, the only mineral present in the domain is calcite. The dominant carbonate species, for the initial pH value, is HCO_3. The incoming fluid does not contain any carbonate species, has a lower pH, and contains dissolved Mg. As the incoming fluid moves into the system, the pH is lowered and calcite dissolves since the solution becomes undersaturated with respect to this mineral.

For case A, although not shown here, simulation indicates that the calcite dissolution front has progressed from the inflow boundary along to fracture to a distance equal to 1.1 m. The calcite dissolution front also corresponds to the dolomite precipitation front along the main fracture. A dolomite dissolution front is also present at x = 0.3 m, upstream of the precipitation front. For case B, the same dissolution and precipitation fronts are observed, but their locations are further along the main fracture when compared to case A. For case B, the calcite dissolution front is located approximately at at 1.2 m and the dolomite dissolution front is at 0.4 m. This more rapid advance is caused by the increased velocity in

the upstream section of the main fracture, caused by the additional fractures.

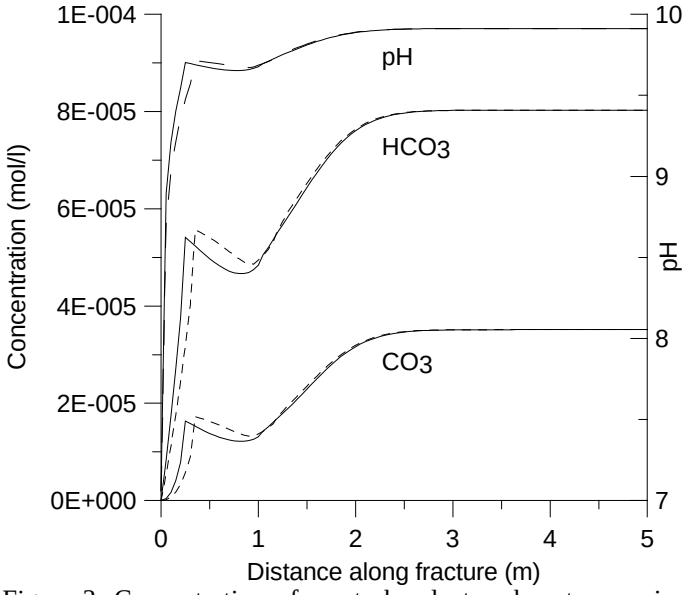

Figure 3. Concentration of most abundant carbonates species and pH along the main fracture (located at y = 0 m). Results from case A are solid lines and results from case B are dashed lines.

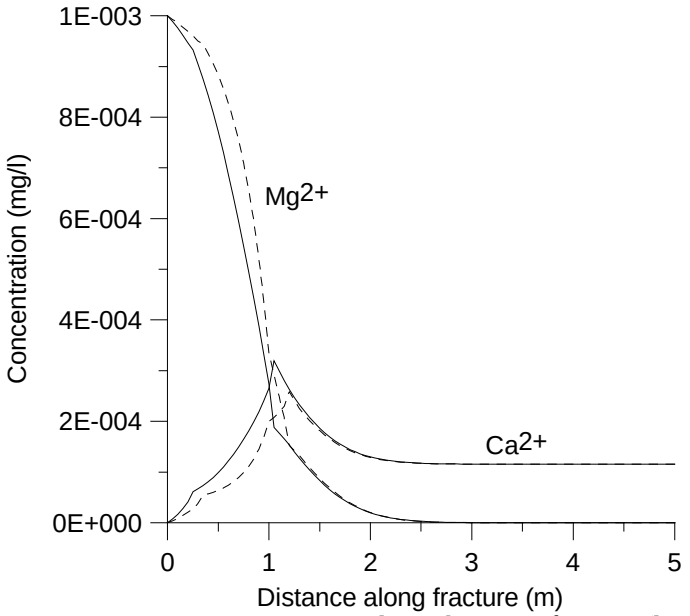

Figure 4. Concentration cations along the main fracture (located at y = 0 m). Results from case A are solid lines and results from case B are dashed lines.

Figure 3 shows the distribution of pH, and the two main carbonate species, HCO_3 and CO_3, along the main fracture. There is a sharp increase in pH and concentrations of the carbonates species around x = 0.3 m, which corresponds to the dolomite dissolution front. Concentration then vary slightly from x = 0.3 to x = 1.1 m, which is the region where dolomite is present. For a distance greater than 1.1 m, which is the region where calcite is present, the concentration gradually rise to the initial value. This rise corresponds to mixing of the incoming fluid with the initial fluid, without any precipitation or dissolution. Similar observations can be made for the calcium and magnesium ions along the fracture (Fig. 4), and for concentrations simulated for case B.

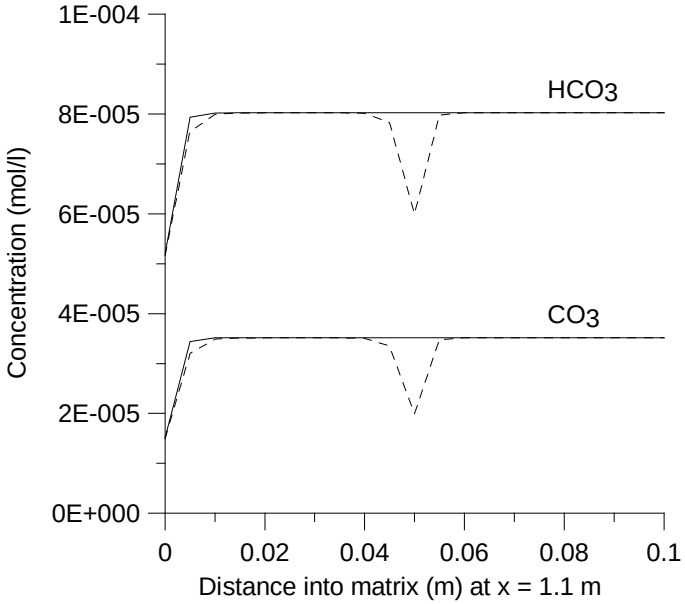

Figure 5. Concentration of most abundant carbonates species in a direction perpendicular to the main fracture (along the y axis, at x = 1.1 m). Results from case A are solid lines and results from case B are dashed lines.

Concentrations simulated perpendicular to the main fractures, and downstream of the fracture oriented along the y-axis, are shown on Figure 5. For case A, the only variation observed into the matrix is near the main fracture and is the result of matrix diffusion. For case B, the incoming fluid has reached the fracture located at y = 0.05 m, which is shown by the decrease in HCO_3 and CO_3 concentrations at y = 0.05 m (Fig. 5). The presence of several interconnected fractures will therefore greatly influence the spatial distribution of chemical species in the fractured porous medium.

Although it is not presented here, the effect of the matrix properties was investigated in a series of different simulations. Simulations for reduced matrix porosity produce a faster migration of the reactive fronts in the fracture, which corresponds to the retardation effect of matrix diffusion shown for non-reactive transport (Therrien & Sudicky, 1996). In the limiting case of a zero-permeability matrix, the reaction front migrates past the outflow of the domain for the same simulation time.

6 CONCLUSION

The model presented in this paper simulates multi-component transport in discretely-fractured porous

media. Flow and transport are simulated in three dimensions in the porous matrix, and they are coupled to 2D flow and transport in fractures. Coupling of the advective-dispersive simulator and geochemical model is done with a two-step iterative process. Chemical reactions can be either at equilibrium or show kinetic effects. A verification example shows that the model can reproduce results already published for the case of an unfractured porous medium. A simplified illustrative example shows the influence of fractures and porous matrix when coupled with multicomponent transport. Interconnected fractures will produce complex flow fields, which will then lead to irregular spatial distribution of chemical species in the fractured system. Matrix diffusion will decrease the migration of reactive fronts.

Improvement needed include the use of more efficient spatial weighting methods, such as flux limiters, for the advective term, enabling the use of coarser simulation grids. Fewer nodes will then be necessary and simulation of larger scale reactive transport problem will be made easier.

The illustrative problem presented here does not test the full capabilities of the model. Future work will focus on field-scale simulations of migration of reactive solute, chemical diagenesis of sediments, and chemical species partition in discretely-fractured geologic materials where chemical and physical transport processes are considered both in the matrix and fracture.

REFERENCES

Engesgaard, P. & K. Kipp 1992. A geochemical transport model for redox-controlled movement of mineral fronts in groundwater flow systems: a case of nitrate removal by oxidation of pyrite. *Water Resour. Res.* 28(10):2829-2843.

Ghogomu, N.F. & R. Therrien 1999. Three-dimensional simulation of mass transport of multiple chemicals in discretely-fractured media. *Program with abstracts GAC-MAC Annual meeting*, vol 24.

Leeming, G.J.S., K. U. Mayer & R.B. Simpson 1998. Effects of chemical reactions on iterative methods for implicit time stepping. *Advances in Water Resources* 22(4):333-347.

Liu, W.C. & T. N. Narasimhan 1989. Redox-controlled multiple-species reactive chemical transport 2. Verification and application. *Water Resour. Res.* 25(5):883-910.

Morel, F.M.M. 1983. *Principles of aquatic chemistry*. New York: Wiley.

Novak, C. F. 1996. Development of the FMT chemical transport simulator: coupling aqueous density and mineral volume fraction to phase composition. *J. Contam. Hydrol.* 21:297-310.

Schäfer, D., W. Schäfer & W. Kinzelbach 1998. Simulation of reactive processes related to biodegradation in aquifers 1. Structure of the three-dimensional reactive model, *J. Contam. Hydrol*. 31:167-186.

Steefel, C.I. & K.T.B. MacQuarrie 1996. Approaches to modeling of reactive transport in porous media. In: Lichtner, P. C., Steefel, C. T., Oelkers, E.H. (Eds.) *Reactive Transport in Porous Media, Reviews in Mineralogy* 34, Mineral. Soc. Am., 83-129.

Steefel, C. I. & P. C. Lichtner 1994. Diffusion and reaction in a rock matrix bordering a hyperalkaline fluid-filled fracture. *Geochim. Cosmochim. Acta* 58:3595-3612.

Steefel, C. I. & P. C. Lichtner 1998a. Multicomponent reactive transport in discrete fractures: I. Controls on reaction front geometry. *J. Hydrol.* 209:186-199.

Steefel, C. I. & P. C. Lichtner 1998b. Multicomponent reactive transport in discrete fratures II: Infiltration of hyperalkaline groundwater at Maqarin, Jordan, a natural analogue site. *J. Hydrol.* 209:200-224.

Stumm, W. & J. J. Morgan 1981. *Aquatic Chemistry.* New York: Wiley.

Therrien, R. & E. A. Sudicky 1996. Three-dimensional analysis of variably saturated flow and solute transport in discretely fractured porous media. *J. Contam. Hydrol*. 23:1–44.

VanderKwaak, J.E., P.A. Forsyth, K.T.B. MacQuarrie & E.A. Sudicky 1995. *WATSOLV sparse matrix iterative solver package version 1.01*. Unpublished report, Waterloo Centre for Goroundwater Research, University of Waterloo, Ontario, Canada.

Walter, A. L., E. O. Frind, D. W. Blowes, C. J. Ptacek & J. W. Molson 1994. Modeling of multicomponent reactive transport in groundwater 2. Metal mobility in aquifers impacted by acidic mine tailings discharge. *Water Resour. Res.* 30(11):3149-3158.